Proceedings of the 9th U.S. National and 10th Canadian Conference on Earthquake Engineering
Compte Rendu de la 9ième Conférence Nationale Américaine et
10ième Conférence Canadienne de Génie Parasismique
July 25-29, 2010, Toronto, Ontario, Canada • Paper No 1413

SEISMIC BEHAVIOR OF SEGMENTED BENTS

M. A. ElGawady[1] A. Sha'lan[2] H. Dawood[2]

ABSTRACT

Precast segmental construction technique is an excellent candidate for economic rapid bridge construction in highly congested urban environments and environmentally sensitive regions. This paper presents the seismic behavior of four hybrid frames. Each column of these frames consisted of post-tensioned precast concrete filled fiber reinforced polymer tubes (PPT-CFFT). A fifth monolithic frame was also tested as a reference specimen. The frames were tested under increasing lateral loading cycles in a displacement control. A typical test frame was approximately 60 in. tall and 82 in. wide. The beam was nominally 8 in. wide by 15 in. deep. The columns cross section diameters was 8 in. parameters investigated included different construction details and energy dissipation systems. The PPT-CFFT frames developed lateral strength and deformation capacity higher than those of the monolithic reinforced concrete frame. However, the hysteretic response of the tests specimens showed that, PPT-CFFT specimens dissipated smaller hysteretic energy compared to that of the monolithic reinforced concrete frame.

Introduction

Currently, correctly designed and detailed reinforced concrete structures, under the prevailing capacity design concepts, are anticipated to exhibit inelastic response leading to structural damage and permanent drift at the conclusion of ground motion excitation which requires long-term closure of highways while expensive repairs, or even complete replacements, are carried out. Following the Kobe (Japan 1994) earthquake, over 100 reinforced concrete bridge columns were demolished because their residual drift ratio exceeded 1.75% [Lee and Billington 2010].

Recent research has shown that residual displacement and damage to reinforced concrete structures linked to seismic loads can be minimized by implementing a precast post-tensioning (PPT) construction system. The potentials of this system were highlighted in the U.S. PRESSS research program where a self-centering system when implemented with precast elements demonstrated superior seismic performance (ElGawady et al. 2005).

Segmental precast column construction is an economic option to accelerate bridge construction in regions of low seismicity in the USA. Examples of bridges constructed with segmental columns include the Louetta Road Overpass (SH-249, Texas), Linn Cove Viaduct (Grandfather Mountain, North Carolina), Sunshine Skyway Bridge (I-275, Florida), Varina-Enon Bridge (I-295, Virginia), John T. Collinson Rail Bridge (Pensacola, Florida), Seven Mile Bridge

[1]Assistant Professor, Dept. of Civil Engineering, Washington State University, Pullman, WA 99163
[2]Graduate Research Assistant, Dept. of Civil Engineering, Washington State University, Pullman, WA 99163

(Tallahassee, Florida), and the Chesapeake and Delaware Canal Bridge (St. Georges, Delaware). However, the applications of this construction system in active seismic regions in the USA are limited due to concerns about its seismic response [Kwan and Billington 2003].

A segmental PPT bridge pier will rock back and forth during a ground motion excitation and then re-center upon unloading as a result of the restoring nature of the applied post-tensioning force. This concept has been implemented in a railway bridge in New Zealand. In 1981, the construction of the South Rangitikei Rail Bridge was completed; the bridge piers were designed to lift off of the foundation under seismic loading. Recently, tests showed that PPT segmental columns can safely resist lateral cyclic forces [Chou and Chen 2006, Ou et al. 2006, Hewes and Priestley 2002]. PPT columns were capable of undergoing large nonlinear displacements without experiencing significant or sudden loss of strength. The nonlinear behavior resulted from opening of the interface joints between segments as well as material nonlinearity. Hence, residual displacements and damage at the conclusion of these tests were small compared to typical monolithic reinforced concrete columns. Increasing the post-tensioning force significantly reduced the residual displacement but increase concrete damage.

Tests on post-tensioned precast bridge piers showed limited hysteretic energy dissipation [Chou and Chen 2006, Hewes and Priestley 2002]. To overcome this drawback, the post-tensioned precast piers were supplied by internal mild steel at the interfaces between the segments as well as between the bottom segment and foundation. However, the provided mild steel increased the residual displacements and damage compared to columns without mild steel. External energy dissipaters "fuses" were also used for bridge piers [Marriott et al. 2009, Rouse 2009, Chou and Chen 2006]. These external simple yield-dissipaters significantly increased the energy dissipation. Another approach to improve the seismic performance of PPT bridge piers is to use a neoprene pads between the pier and its foundation. ElGawady et al. (2005 and 2006) showed that there is an interaction between the rocking response and the foundation interface material. Using soft rubber above a reinforced concrete base significantly reduced the velocity demand on the column. The energy dissipation increased as well since the soft rubber changed the energy dissipation function from a discrete to a continuous function.

Recently, concrete filled fiber reinforced polymer tubes (CFFT) has been successfully used as pier columns, girders, and piles in different field applications by several State Departments of Transportations [Fam et al. 2003]. Zhu et al. [2006] investigated the seismic behavior of one PPT concrete column encased in concrete filled fiber reinforced polymer tubes (PPT-CFFT). The column reached a drift of 13% without losing its strength and the test was stopped because the actuator reached its displacement capacity. ElGawady and Booker [2009] and ElGawady et al. [2010a and 2010b] investigated the cyclic behavior of 1/5 scale hybrid segmental bridge piers consisting of precast post-tensioned concrete filled fiber reinforced polymer tubes (PPT-CFFT).

Experimental Work

Specimens Description

This study investigates the cyclic behavior of five moment resisting frames (Table 1, Fig.1). A typical test frame was approximately 60 in. tall and 82 in. wide (Fig. 2). The beam was 8 in. wide by 15 in. deep. The columns had a diameter of 8 in. To provide fixity at the bottom, a reinforced concrete foundation 16 in. wide, 24 in. thick, and 26 in. long was constructed and post-tensioned to the lab strong floor prior to testing. The beam clear span was 66 in. and the

column clear height was 45 in. The concrete used for specimens F-FRP3-S and F-FRP3-R had a compressive strength of 2973 psi and a modulus of elasticity of 2167 ksi. The other specimens were using concrete having a compressive strength of 2068 psi and modulus of elasticity of 1975 ksi. The foundations of specimens PPT-CFFT were leveled using 0.25 in. thick grout.

Table 1. Summary of the test specimens

Specimen	Joints	Energy dissipater	No. of FRP segments per column	FRP segment height (in)	Reinforcement	
					Longitudinal	Horizontal
F-RC	Monolithic	--	--	--	6 No. 3	No. 2 spiral
F-FRP1	Dry	--	1	45	PT* Bar	GFRP
F-FRP3	Dry	--	3	15	PT* Bar	GFRP
F-FRP3-S	Dry	Steel angles	3	15	PT* Bar	GFRP
F-FRP3-R	Rubber	--	3	15	PT* Bar	GFRP

Diameter of the column = 8 in., the height of the load above the top of the footing was 52.5 in. for all specimens

* PT: post-tension

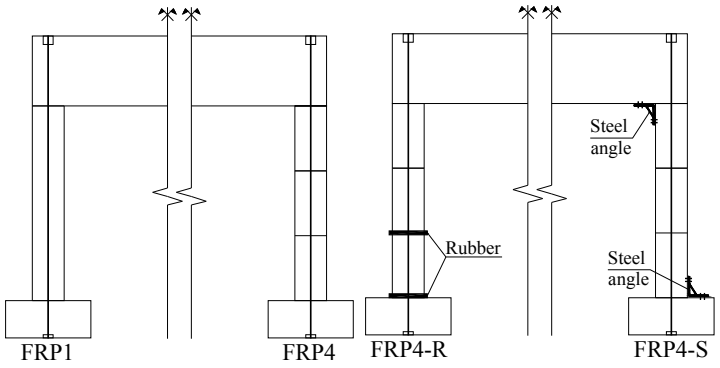

Figure 1. Schematic of the FRP test specimens.

Specimen F-RC was designed and constructed according to ACI 318-08 as a special moment resisting frame. Each column of the frame was provided with six No. 3 Grade 60 (with measured yield strength of 63 ksi) as longitudinal reinforcement. Shear and confining reinforcement was provided by a No. 2 Grade 40 (with a measured yield strength of 54 ksi) spiral at a pitch of 3.5 in. These represent a longitudinal reinforcement ratio of 1.31% and a transverse volumetric reinforcement ratio of 0.7%.

Each column in the other four PPT-CFFT specimens was constructed by stacking precast concrete filled fiber reinforced polymer tube (CFFT) segments one on top of the other and then connecting the assembly structurally with unbonded post-tensioned Dywidag bar passing through PVC duct located within the segments. Each column in specimen F-FRP1 was constructed using a single CFFT segment. Each column in the other PPT-CFFT specimens was constructed using three segments of CFFT.

The four PPT-CFFT specimens utilized off-the-shelf circular glass fiber reinforced

polymer (GFRP) tubes as shear and confining reinforcement as well as a stay-in-place casting forms for the columns. The GFRP tubes were made by filament-winding technique with ±55° fiber orientation with respect to the longitudinal axis of the tube. Each tube was constructed by stacking 10 layers of E-glass fibers and epoxy resin each having a thickness of approximately 0.0125 in. The tube had a nominal wall thickness of 0.125 in. and interior diameter of 8 in. The tube had a measured tensile strength and elastic tensile modulus of 9200 psi, and 2008 ksi, respectively (ASTM D3039M-08, ASTM 2008b).

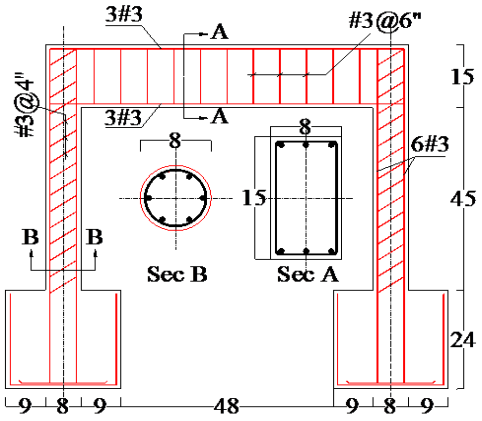

Figure 2. Concrete dimensions and reinforcement of the monolithic frame.

A PPT-CFFT specimen did not posses any reinforcement but a post-tensioning high strength Dywidag bar and the GFRP tube. A 2 in. polyvinyl chloride (PVC) duct, to allow for the post-tensioning bar, was placed in the center of the tube prior to casting. The wall thickness of the GFRP tube was designed using the guidelines given in ACTT-95/08 (Seible et al. 1995) to avoid brittle shear failure. The applied post-tensioning force, after initial losses, was 33.9 kips corresponding to 18% of the ultimate strength of the post-tensioning bar. This value was selected such that specimens FRP-1, FRP4, and RC had approximately the same nominal lateral strength. For Specimen F-FRP1 and to avoid direct contact between the end of the FRP tube and the adjacent footing, the height of the GFRP tube was shorter than the column height by 0.125 in. to allow the column rotation without damage to the GFRP tube edge.

Specimen F-FRP3-R had neoprene pads placed at the interface between the footing and bottom segment, as well as between the last segment and the cap beam. Two 9 in. square sheets each having 0.5 in. thickness were placed at each of these locations for a total thickness of 1 in. The neoprene was used to decrease the lateral stiffness of the column leading to a lengthening of the natural period of the column which potentially reduces the seismic demand in the case of a real earthquake scenario. A commercial neoprene with a durometer hardness of 40 (ASTM D2000-08, ASTM 2008c) was used. The neoprene was tested in compression according to ASTM D575-91 (ASTM 2007). Fig. 2 shows the stress-strain curve of the neoprene used during this research.

Specimen F-FRP3-S had two A36 steel angles attached to the base and bottom segment of the column in the loading plane (Fig. 1). The angles (Fig. 4) were approximately 4 in. wide and the legs were each 5 in. long and approximately 0.40 in. thick. Two holes in one leg and three holes in the other leg were drilled to allow attachment to the footing, beam, and column segment. The angles were attached to the footing, beam, and column segments using 0.40 in.

threaded rods and nuts anchored into the concrete with the Hilti HIT-RE 500 epoxy system. However, during bolting the angle at the northern joint to the beam, only 2 bolts instead of 3 were used. During pouring the concrete beam, one stirrup disoriented from its original position blocking the passage of the third bolt. Plastic deformations and yielding of these sacrificial steel angles would contribute to the dissipation of the input seismic energy which would reduce the seismic displacement demand on the frame in the case of a real earthquake scenario.

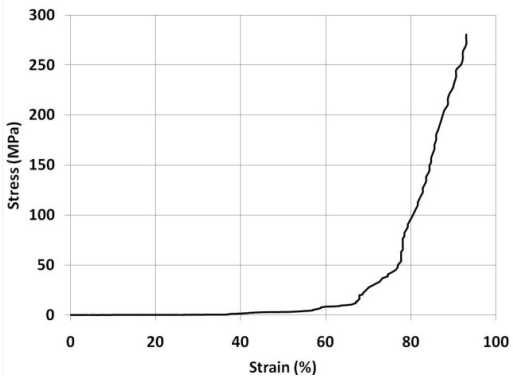

Figure 3: Stress-strain curve of the neoprene

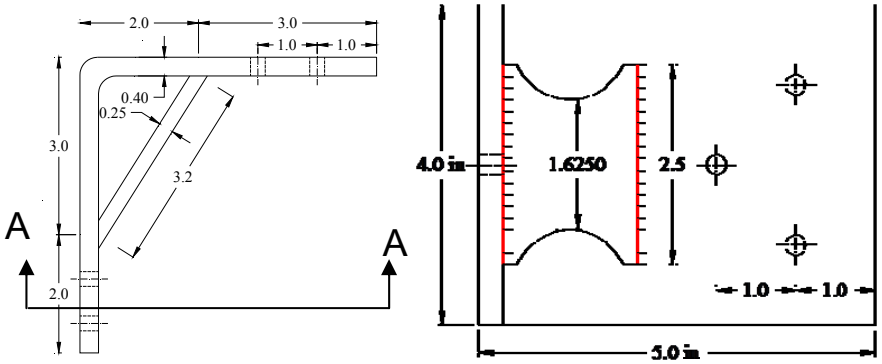

Section (A-A)

Figure 4: Detailed of the steel angle (All dimensions are in inches)

Test Setup And Loading Pattern

The specimens were subjected to reverse cyclic lateral loading with increasing levels of lateral displacements. The lateral load was applied using a horizontally-aligned servo-controlled hydraulic loading actuator positioned at the top beam centerline. This actuator was anchored against a strong steel frame. The actuator has a load capacity of 22 kips and a stroke capacity of ±5 in. (Fig. 4). Lateral loads were applied under displacement control based on a pattern of progressively increasing displacements, referenced to the horizontal displacement to cause first yield (Δ_y) in the longitudinal reinforcement of the monolithic column. The loading pattern for the specimens consisted of three cycles at displacement levels of ±0.5, ±1, ±1.5, ±2, ±2.5, ±4, ±5, and ±6 times Δ_y.

Instrumentation

The lateral displacements at the column top, the vertical displacements at different

heights of each column, the applied post-tensioning force and lateral force, and circumferential and longitudinal strains in the GFRP tubes at different locations were measured with a frequency of 2 Hz.

Experimental Results and Discussion

General Performance

The monolithic specimen reached an ultimate strength of approximately 11.9 kips. Several minor flexural cracks started at the column top at a drift angle of 0.8%. These cracks extended to the beam in the form of shear cracks at a drift angle of 2.7% (Fig. 5). Significant concrete spalling occurred at the beam-column and foundation-column joints at a drift of 5.1% followed by longitudinal bar buckling. Concrete spalling occurred at the beam-column and foundation-column joints over a length ranging from 4 to 7 in. Cycling continued leading to substantial longitudinal bars buckling. Crushing of the concrete core at the beam-column and foundation-column joints appeared at a drift of 6.9%. Finally, the spiral reinforcement of the northern column fractured at a displacement level of 7.2% and a load of 7.3 kips.

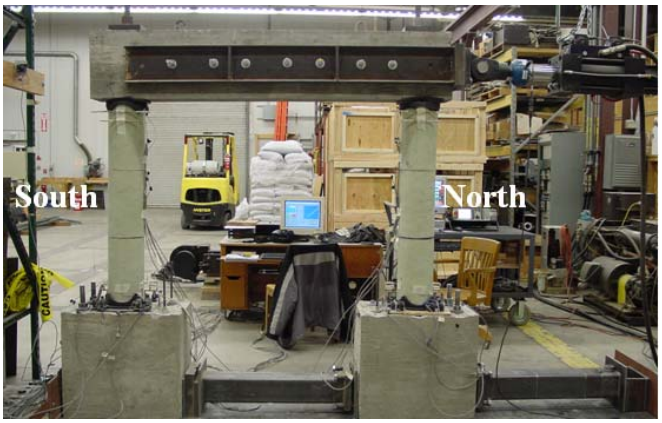

Figure 5: Specimen F-FRP3-R ready for testing

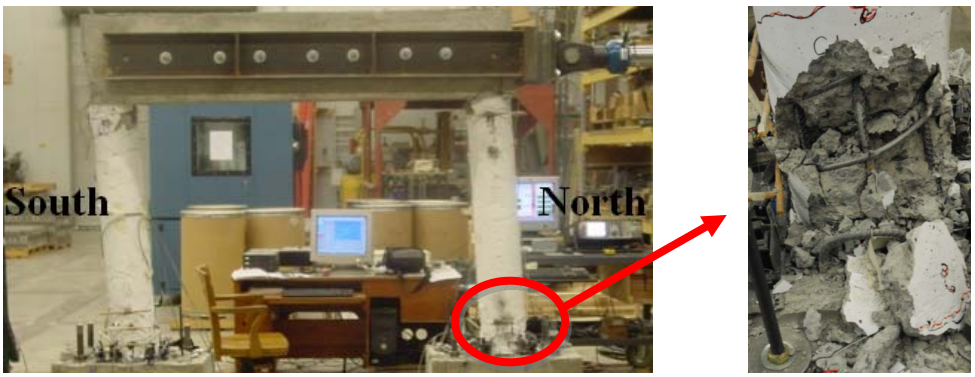

Figure 6: Specimen F-RC during and after testing

Specimens F-FRP1 and F-FRP3 similarly behaved. Specimens F-FRP1 and F-FRP-3 reached peak lateral forces of approximately 22.9 and 23.9 kips, respectively. The peak lateral

forces occurred at a drift angle of 9.3% for both specimens. At such displacement the actuator reached its stroke displacement capacity and no failure of the specimens was recorded. The grout layers on top of the foundations significantly cracked and crushed during testing. The FRP tube suffered very minor damage in several spots at the interface joints in both specimens. For F-FRP3 (Fig. 7), no openings of the interface joints between the segments were observed. However, the interface joints at the column top and bottom opened and the FRP tube beard against the concrete beam and foundation during the rocking mechanism. At a drift angle of 8.1%, local damage in the FRP matrix occurred at the top 2 in. in both columns of specimen F-FRP3. However, the bottom did not suffer any type of visual damage. For F-FRP1 (Fig. 6), since the height of the FRP tubes were shorter than the column height, the FRP tubes did not come into contact with the base; hence, no tube damage was observed at the bottom interface joints. At the top interface joint of the northern column, limited damage in the FRP matrix occurred due to bearing of the FRP tube against the concrete beam. No visual damage occurred at any other interface joints. In both frames no concrete crushing was observed.

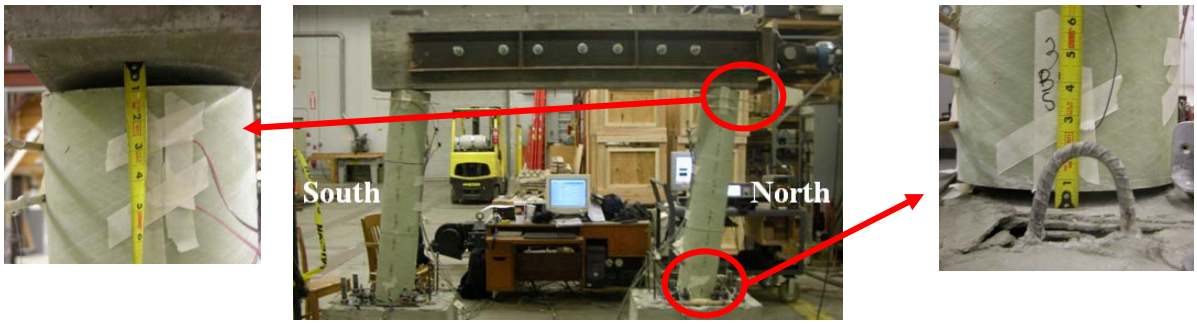

Figure 7: Specimen F-RC during and after testing

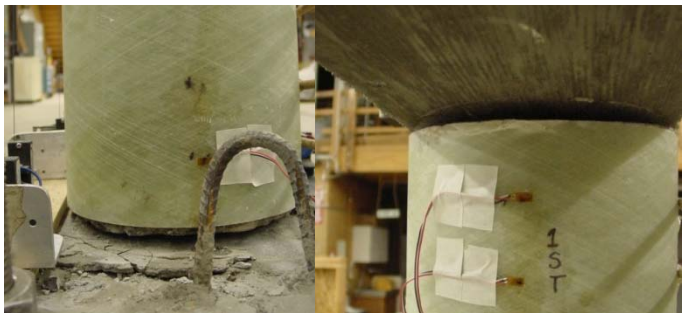

Figure 8: Opening of the top and bottom interface joints for the north column of Specimen F-FRP1

Specimen F-FRP3-R behaved nonlinear due to the hysteretic deformations in the neoprene. However, the segments did not experience any type of damage. The specimen reached a peak lateral load of 7.4 kips at a drift angel of approximately 8.9%. No openings of the interfaces between the segments were observed. However, the interface joints at the column top and bottom opened. Also, no damage to the grout layer was observed thanks to the existence of the neoprene layers. After finishing the test, minor rupture in the rubber pads were observed; however, this may happened during the post-tensioning process.

The performance of Specimen F-FRP3-S in the positive loading direction was different

from the negative loading direction. The peak strength in the positive direction was 25.2 kips at a drift angle of 6.4%. The peak strength in the negative direction was 26.6 kips at a drift angle of 8.9%. This asymmetric response linked to the asymmetry in fixing the fuse angles as discussed before. During the first loading cycle of the specimen to a drift angle of 2.4%, a splitting shear crack began at the bottom surface of the reinforced concrete beam at the northern column. At a drift angle of 4%, a diagonal crack appeared in the beam at the southern column. At the end of the 6.5% drift angle, the bolts at the northern column pulled out from the concrete beam as well as spalling of the concrete cover exposing the beam longitudinal reinforcement (Fig. 9(a)). Cycling continued and by the end of a drift angle of 7.2%, bolts fixing the fuse steel angles to the southern column segments began to pull out of the column leading to cracking of the FRP tube at the upper and lower segments. The cracking occurred parallel to the direction of the main fiber i.e. at approximately 53° (Fig. 9(b)). At a drift angle of approximately 9.4% the actuator reached its stroke displacement capacity and the test was stopped (Fig. 9(c)). During the last cycle, the lateral resistance of the test frame dropped to 82% of the frame ultimate strength. Similar to the other segmented frames, no opening of the segment to segment interface joints was observed during testing.

(a) (b) (c)

Figure 9: The beam-column joint at different drift angles: (a) 6.5% (Northern Column), (b) 9.1% (Southern Column), and (c) 9.4% (Northern Column)

Hysteretic Behavior

The lateral forces vs. the lateral displacements at the centerline of the beam for each test specimen are shown in Fig. 8. Specimen F-RC displayed approximately a linear performance until first yield, which was then followed by stable nonlinear symmetrical hysteretic loops through a drift of approximately 7.6%. The nonlinearity was mainly due to flexural concrete cracking, significant spalling, longitudinal bar yielding and buckling, spiral reinforcement rupture, and concrete crushing. A good feature of the hysteretic of this specimen is the large area contained in the hysteretic loops, indicating significant energy dissipation during testing. Another characteristic of the loops was a significant residual displacement, which increased with increasing imposed lateral displacement. The specimen resisted the maximum lateral load for several cycles with minor strength degradation.

All the PPT-CFFT specimens except FRP4-R developed a lateral strength significantly higher than the reference F-RC specimen and were able to sustain the peak lateral load for several cycles at higher drifts with limited visible signs of damage. The hysteretic loops for specimens F-FRP1, and F-FRP3 were very similar with stable nonlinear characteristics. The residual displacement was small compared to specimen F-RC; the PPT-CFFT system was self-centering. This characteristic is typical of a rocking frame where the frame approximately

resumes its original position upon unloading as a result of the restoring nature of the post-tensioning force. Another feature of the loops is the stiffness softening with very limited damage due to opening of the interface joints at the base and the top of the columns as described earlier. Another feature for rocking is the narrow hysteresis loops indicating limited energy dissipation during the test. Specimen F-FRP3-S showed a larger hysteretic loops indicating higher energy dissipation. Thanks to the steel angles. The hysteretic loops for specimen F-FRP4-R show a minor nonlinear response due to nonlinear deformations in the neoprene.

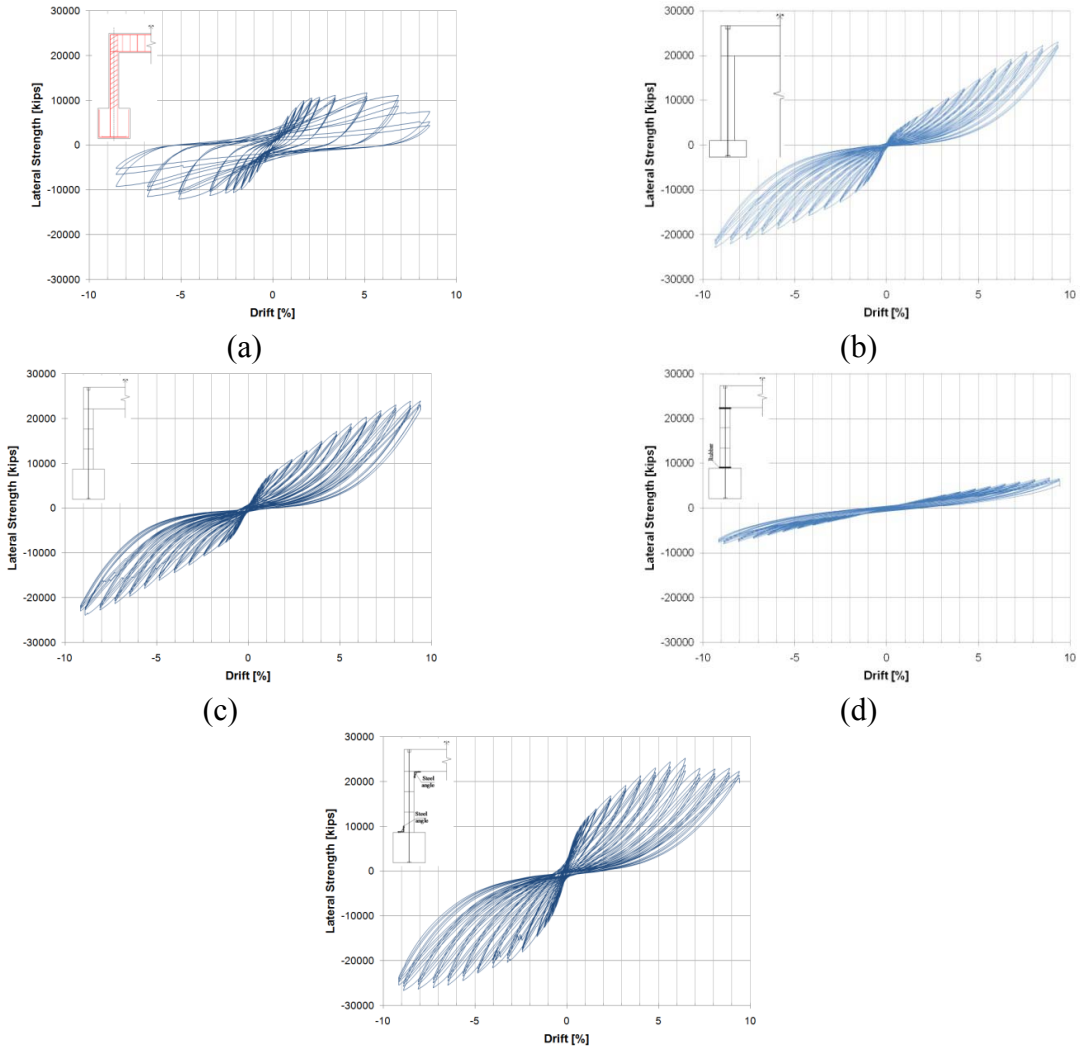

Figure 10. Hysteretic curves for the tests specimens (a) F-RC, (b) F-FRP1, (c) F-FRP3, (d) F-FRP3-R, and (e) F-FRP3-S.

Summary and Conclusions

Five concrete frames were tested during the course of this research. The first frame was designed and constructed as a monolithic special moment resisting frame. The columns of the other four frames were constructed using PPT-CFFT segments. Based on the results of this experimental investigation, the following conclusions and findings are drawn:

- The PPT-CFFT can safely and effectively resist lateral cyclic forces. The frames were capable of undergoing large nonlinear displacements without experiencing significant or sudden loss of strength. The tested PPT-CFFT and the RC specimens behaved in a nonlinear ductile manner. All the PPT-CFFT specimens achieved a drift of approximately 9.5% with no failure. This was different from the RC specimen which failed at drift angle of 6.9%.
- Damage in all the PPT-CFFT specimens except specimen F-FRP3-S was very minor compared to the damage in the RC specimen. PPT-CFFT suffered minor damage in the GFRP tube associated with bearing of the segments against the concrete beam. Specimen F-FRP3-S had severe damage in the beam due to pull out of the fuse angle as well as cracking in the FRP tube. Damage in the RC specimen was in the form of rebar buckling and yielding as well as concrete cover spalling.
- At high drifts, all PPT-CFFT columns had residual displacement significantly lower than those of the conventional RC column.

References

Chou, C. and Chen, Y. 2006. Cyclic tests of post-tensioned precast CFT segmental bridge columns with unbonded strands, *Earthquake engineering and structural dynamics*, 35, 159-175.

ElGawady M., Booker, A., Dawood H. (2010a). Seismic behavior of post-tensioned concrete filled fiber tubes, ASCE, *Composites for Construction J.*

ElGawady, M. A., Dawood, H. (2010b). Lateral Performance Of Precast Post-Tensioned Concrete Filled Fiber Tubes, *proceeding of the 9th US National and 10th Canadian Conf. Earth. Eng.*, Toronto

ElGawdy M., Booker, A. (2009). Static cyclic response of concrete filled fiber tubes, *proceeding of FRPRCS-9*, Sydney, Australia

ElGawady M., Ma Q., Ingham J., Butterworth J. 2006. The effect of interface material on the dynamic behavior of free rocking blocks, *8th NCEE*, EERI, San Francisco, CA.

ElGawady M., Ma Q., Ingham J., Butterworth J. 2005. Experimental investigation of rigid body rocking, *The New Zealand Concrete Ind. Conf.*, Auckland, 2005, p.1-8

Fam, A. Pando, M, Filz, G. and Rizkalla, S. 2003. Precast piles for Route 40 Bridge in Virginia using concrete-filled FRP tubes, *PCI journal,* 48(3), 32-45.

Hewes, J. T.; and Priestley N., 2002. Seismic design and performance of precast concrete segmental bridge columns, *Report No. SSRP-2001/25*, Univ. of California at San Diego.

Kwan, W.; and Billington, S. 2003. Unbonded posttensioned concrete bridge piers I: monotonic and cyclic analyses, *Journal of Bridge Engineering*, 8 (2), 92- 101

Lee, K.; and Billington, S. In print. Residual Displacement Prediction for Structural Concrete Columns under Earthquake Loading, ASCE, *J. Bridge Engineering*

Marriott, D.,Pampanin, S., Palermo, A., 2009. Quasi-static and pseudo-dynamic testing of unbonded post-tensioned rocking bridge piers with external replaceable dissipaters, *Earthquake Engineering & Structural Dynamics*, 38(3).

Ou, Y.; Chiewanichakorn, M.; Ahn, I.; Aref, A.; Chen, S.; Filiatrault, A.; and Lee, G. 2006. Cyclic performance of precast concrete segmental bridge columns, *TRB J.*, 1976, 66-74 pp.

Seible, F., Priestley, M. J. N., Chai, Y. H. 1995. Earthquake Retrofit of Bridge Columns with Continuous Carbon Fiber Jackets, *Advanced Composites Technology Transfer Consortium*, Report No. ACTT-95/08, La Jolla, California.

Rouse, J., 2009. Self-Centering Bridge Piers with Structural Fuses, *Mid-Continent Transportation Research Symposium*, Ames, Iowa.

Zhu, Z., Ahmad, I., and Mirmiran, A., 2006. Seismic Performance of Concrete-Filled FRP Tube Columns for Bridge Substructure, *Journal of Bridge Engineering* 11 (3), 359-370.